applied sciences

MDPI

Article

# Improvement of ANFIS Model for Prediction of Compressive Strength of Manufactured Sand Concrete

**Hai-Bang Ly [1], Binh Thai Pham [1,*], Dong Van Dao [1,*], Vuong Minh Le [2], Lu Minh Le [2] and Tien-Thinh Le [3,*]**

[1] University of Transport Technology, Hanoi 100000, Vietnam
[2] Faculty of Engineering, Vietnam National University of Agriculture, Gia Lam, Hanoi 100000, Vietnam
[3] Institute of Research and Development, Duy Tan University, Da Nang 550000, Vietnam
* Correspondence: binhpt@utt.edu.vn (B.T.P.); dongdv@utt.edu.vn (D.V.D.); letienthinh@duytan.edu.vn (T.-T.L.)

Received: 27 August 2019; Accepted: 09 September 2019; Published: 12 September 2019

**Featured Application: Authors are encouraged to provide a concise description of the specific application or a potential application of the work. This section is not mandatory.**

**Abstract:** Use of manufactured sand to replace natural sand is increasing in the last several decades. This study is devoted to the assessment of using Principal Component Analysis (PCA) together with Teaching-Learning-Based Optimization (TLBO) for enhancing the prediction accuracy of individual Adaptive Neuro Fuzzy Inference System (ANFIS) in predicting the compressive strength of manufactured sand concrete (MSC). The PCA technique was applied for reducing the noise in the input space, whereas, TLBO was employed to increase the prediction performance of single ANFIS model in searching the optimal weights of input parameters. A number of 289 configurations of MSC were used for the simulation, especially including the sand characteristics and the MSC long-term compressive strength. Using various validation criteria such as Correlation Coefficient (R), Root Mean Squared Error (RMSE), and Mean Absolute Error (MAE), the proposed method was validated and compared with several models, including individual ANFIS, Artificial Neural Networks (ANN) and existing empirical equations. The results showed that the proposed model exhibited great prediction capability compared with other models. Thus, it appeared as a robust alternative computing tool or an efficient soft computing technique for quick and accurate prediction of the MSC compressive strength.

**Keywords:** manufactured sand concrete; adaptive neuro fuzzy inference system; compressive strength; teaching-learning-based optimization; mixture proportion; principal component analysis

## 1. Introduction

In recent years, manufactured sand has been progressively used to replace natural sand in building materials [1]. This new type of material, produced by crushing rock depositions, exhibits some morphology features that are unique and cannot be found in natural sand, such as the angular and rougher texture [2,3]. Unlike manufactured sand, the common negative characteristic while using natural sand in concrete is the alkali-silica reactions between the reactive silica components and the alkali hydroxides derived from the cement. Such reactions lead to the expansion, deterioration and even failure of concrete structural elements [4]. On the contrary, using manufactured sand is advantageous with the possibility of preselection of low silica content rocks as to avoid such alkali-

silica reactions. Besides, manufactured sand could positively influence the strength and durability of concrete, mainly due to better interlocking between highly irregular particles [2] or a better bonding between steel bar and concrete [5]. Indeed, as demonstrated by Li et al. [6] in an experimental investigation, machine-made sand particles exhibit usually a higher degree of angularity than river sand particles (i.e., in terms of morphology). The same conclusion was also achieved by Li et al. [6] in terms of surface texture. Logically, they found that the compressive and flexural strengths of pavement cement concrete, as well as its abrasion resistance, have been largely improved compared to conventional sand concrete. Various other comparative studies have been introduced in the literature in proving the performance of machine-made sand such as Gonçalves et al. [7], Yamei et al. [8] or Mundra et al. [9]. Therefore, manufactured sand has currently caught great attention from researchers, as well as the whole construction industry [10,11].

In the literature, many works have focused on the quantification of how the concrete workability and durability could be influenced by using manufactured sand [6,12], especially its compressive behavior [1,11,13–15]. In a series of papers, Shen et al. [3,13] have identified the influence of the shape of manufactured sand and roughness on the concrete compressive strength based on digital image analysis and experimental compression tests. The authors have also pointed out that the stone powder of manufactured sand exhibited a considerable effect on the performance of concrete. In another study, Li et al. [6] have prepared manufactured sand concrete (MSC) samples from different petrographic sands such as limestone, quartzite, granite, basalt and granite gneiss, respectively. The authors discovered that morphology and texture characteristics of manufactured sand hugely influenced the performance of concrete. As an example of results, the flexural strength and abrasion resistance of MSC were better than natural sand concrete if the crushing value of manufactured sand particles is less than 26.5%. It was also proven in many other experimental studies that MSC exposed better compressive behavior than that composed of natural river sand [16,17].

One of the most important parameters of MSC is the compressive strength, which is often obtained by experimental laboratory tests. However, these laboratory investigations were generally complexes, cost and time consuming. Moreover, the laboratory tests were often limited within 90–180 days periods [18]. Despite all the efforts, it was not often possible to perform too many variations of ingredients (i.e., proportion of cement, water and machine-made sand as well as stone powder content in sand). Recently, Artificial Intelligence (AI) based methods have been successfully employed in the field of materials [19], especially for predicting compressive strength of concrete [20–24]. Dao et al. [25,26] have proposed a comparative study between Adaptive Neuro Fuzzy Inference System (ANFIS), Artificial Neural Networks (ANN) and Support Vector Machine (SVM) in predicting the compressive strength of geo-polymer concrete based on mixture inputs. Similarly, Golafshani et al. [27] has optimized the mix design of silica fume concrete in order to obtain desired compressive strength using Biogeography-based programming. In another study, Bingöl et al. [28] has shown that the ANN model provided more accurate results than traditional regression in predicting compressive strength of lightweight concrete under heat treatment. Mishra et al. [29] has used ANN and ANFIS for investigating the compressive strength of brick–mortar masonry. In combining AI methods with global optimization techniques, Bui et al. [30] have implemented whale algorithm in order to better optimize the weight of a ANN model when predicting compressive strength of concrete. In another attempt, Behnood et al. [31] have also predicted compressive strength of silica fume concrete based on a hybrid model involving ANN and multi-objective grey wolves technique. Based on these mentioned studies, it can be stated that the AI based methods could be able to analyze the nonlinear relationship between ingredients and compressive strength of various types of concrete for better prediction and assessment [32–36].

In this study, the main objective is to improve the performance of individual ANFIS model, which is one of the effective AI models, by using two optimized techniques namely Principal Component Analysis (PCA) and Teaching-Learning-Based Optimization (TLBO) for better prediction of the compressive strength of MSC. Out of these optimized techniques, PCA technique was applied for reducing the noise in the input space whereas TLBO was employed to increase the prediction performance of single ANFIS model in searching the optimal weights of input parameters. A number

of 289 compression tests of MSC were gathered from the available literature, including inputs parameters such as mixture proportions, cement's compressive strength, water content, as well as manufactured sand's characteristics. The target response of the present study is the long-term compressive strength of MSC, ranging from 3 to 388 days of curing age. Correlation Coefficient (R), Root Mean Squared Error (RMSE) and Mean Absolute Error (MAE) were employed to validate and test the effectiveness of the proposed model, as well as to compare with other AI models such as individual ANFIS and ANN.

## 2. Research Significance

As indicated in the introduction part, the estimation of the compressive strength of MSC is important in civil engineering applications. Although miscellaneous experimental investigations have reported this problem, it is difficult to deduce a generalized formulation, taking into account all the parameters that affect compressive strength of MSC, especially in terms of sand's characteristics. The employment of AI approaches could help to look into the (nonlinear or not) relationships between the desired outputs and the corresponding inputs. That way, the influence on the MSC's compressive strength of input variables, particularly sand's characteristics, could be fully achieved and quantified. Moreover, pre-processing data technique such as PCA and optimization technique namely TLBO could be applied to improve the performance of a popular ANFIS model for better accurate prediction of the compressive strength of MSC. Thus, it can be a great approach which could help engineers and/or researchers to decrease cost and time in laboratory experiments for determination of the compressive strength of MSC.

## 3. Materials and Methods

### *3.1. Adaptive Neuro Fuzzy Inference System (ANFIS)*

Early introduced in the 1990s by Jang [37], ANFIS is well-known as a hybrid AI model in merging ANN [38–41] and Fuzzy Logic (FL) [42]. The ANFIS architecture consists of five principal layers such as fuzzification, rule, normalization, defuzzification and aggregation [37,43–46]. Based on such construction, the neural network exhibits the ability to identify the parameters of FL algorithm [47–49]. In ANFIS, the Takagi–Sugeno if–then rules and appropriate membership function are employed for the fuzzy inference system [50,51]. Similar to ANN, hybrid ANFIS technique has also an ability to identify the nonlinear relationship between inputs and outputs [43,52,53]. It is worth noticed that ANFIS exhibits a better prediction efficiency than individual ANN or FL, as demonstrated in several investigations, such as in the works of Mukerji Aditya et al. [54] or Nayak et al. [55]. However, there are several limitations in ANFIS model such as ANFIS is not powerful in searching the best firing strength (i.e., weight) [56,57], which greatly impact the prediction effectiveness [47]. Various investigations have employed different optimization methods to find the weighs of parameters in a better way, for instance using Genetic Algorithm, Particle Swarm Optimization, Grey Wolf Optimizer or Invasive Weed Optimization [58–63]. In this paper, we proposed the Teaching-Learning-based Optimization (TLBO) to optimize the parameter's weights in ANFIS.

### *3.2. Teaching-Learning-Based Optimization (TLBO)*

TLBO is an optimization technique that is recently introduced for solving scheduling problems [64–66]. As the name indicated, TLBO includes two main phases: the "Teacher Phase", where the model learns something from a teacher and the "Learner phase", where the model learns itself by interacting with other learners. The structure of TLBO can be divided in three main steps as the followings [67–70]:

#### 3.2.1. Initialization of the Population

In this step, a population of size N is generated along with the initial parameters such as number of jobs or number of machines. Each element in the population is considered as a student in a class.

3.2.2. Teacher Phase

In this step, the main objective of the teacher is to increase the mean result of the class in a subject based on each student's capability. Let us define "kbest" is the best learner in the class and $X_{kbest}$ is the highest overall result in the entire class in all subjects. The mean result of the class can be improved using the difference between the current mean result and the result given by the teacher such as:

$$Diff = r_i \left( X_{kbest} - T_F M_{j,i} \right), \quad (1)$$

where $r_i$ is a random number chosen between 0 and 1, $T_F$ is the teaching factor and $M_{j,i}$ is the mean of all learner's results in subject $j$ at iteration $i$.

The current solution is then updated using the following equation:

$$X_i^{'} = X_i + Diff, \quad (2)$$

where $X_i$ is the current solution at iteration $i$ and $X_{i'}$ is the updated solution. If the updated solution gives a better function value, then accept it, otherwise keep the current solution.

3.2.3. Learner Phase

In this step, the learners increase their results by interacting between themselves. Considering two learners A and B, the solution is updated using the following relations:

$$X_{j,i,A}^{"} = X_{j,i,A}^{'} + r_i \left( X_{j,i,A}^{'} - X_{j,i,B}^{'} \right) \text{ if } X_{j,i,A,total}^{'} < X_{j,i,B,total}^{'}, \quad (3)$$

$$X_{j,i,A}^{"} = X_{j,i,A}^{'} + r_i \left( X_{j,i,B}^{'} - X_{j,i,A}^{'} \right) \text{ if } X_{j,i,A,total}^{'} \geq X_{j,i,B,total}^{'} \quad (4)$$

If the updated solution gives a better function value then it is accepted. When the number of generations is completed, then the algorithm is stopped.

*3.3. Principal Component Analysis (PCA)*

In multi-variable problems, particularly in the case of applying AI models, PCA exhibits many advantages in the step of pre-processing data. PCA could help the training phase of AI models in: (i) assessing the feasibility of space reduction when the problem has too many inputs [71,72], (ii) preventing the overtraining, as recommended in the work of Defernez et al. [73], and (iii) reducing the noise in the input data [74–76]. Using PCA technique, important statistical information in the data has been conserved without dropping any typical characteristics [77,78]. The main steps of PCA technique are given below [71,79,80]:

- Preparation and normalization of inputs;
- Calculation of the covariance matrix;
- Calculation of the eigenvalues and eigenvectors;
- Estimation of the proportion of total variance of each principal component;
- Identification of the loading of principal components and contribution of inputs.

In this study, PCA was applied in order to reduce noise in the input space for training the models. Two datasets were prepared: one with raw inputs and the data with PCA pre-processed. These two datasets were used as inputs for the training and testing phases of the models as to demonstrate the effectiveness of PCA technique.

*3.4. Collection of Data*

In this study, the target output is the compressive strength (both cubic and cylinder) of MSC at different curing ages ranging from 3 to 388 days. The database was collected from experimental tests in the available literature [14,81–83]. A number of 289 MSC samples have been mixed by raw materials such as: (i) ordinary silicate cements; (ii) admixture consisted of fly ash, slag and silica fume; (iii) crushed stone and (iv) manufactured sand. The properties of the mentioned materials (i.e., compressive strength and tensile strength of cement at 28 days), the mix proportions as well as MSC's compressive strength were detailed in the database, as summarized in Table 1. A factor of 0.82 was used to convert the cylinder and cubic compressive strength of MSC as suggested by Zhao et al. [83]. As indicated, the cubic compressive strength of MSC, denoted by Y, ranges from 19 to 96.3 MPa, with an average value of 55.80 MPa, a standard deviation of 1670 MPa (corresponding to a coefficient of variation CV of 29.93%). The characteristics of sand such as stone powder content and fineness modulus are also indicated. As reported by Shen et al. [13], stone powder content in sand was most influenced factor on the compressive performance of MSC.

Initial data analysis (histogram) was performed and showed that most inputs, except $I_3$, $I_4$ and $I_9$, are well distributed and suitable for the training of the models (i.e., the histogram is close to a Gaussian distribution). For that reason, PCA was performed in this study to reduce the noise in the 11-dimensional input space. As mentioned above, two datasets were prepared for training the models using the raw and PCA pre-processed inputs. The detailed analysis of PCA technique are indicated in the results and discussions section.

**Table 1.** Statistical analysis of inputs and output used in this study.

| Parameter | Compressive Strength of Cement | Tensile Strength of Cement | Curing Age | $D_{max}$ of Crushed Stone | Stone Powder Content in Sand | Fineness Modulus of Sand |
|---|---|---|---|---|---|---|
| Unit | MPa | MPa | Days | mm | % | [-] |
| Notation | $I_1$ | $I_2$ | $I_3$ | $I_4$ | $I_5$ | $I_6$ |
| Min | 35.50 | 6.90 | 3.00 | 16.00 | 0.00 | 2.20 |
| Average | 47.95 | 8.25 | 80.93 | 28.31 | 7.54 | 3.06 |
| Median | 46.80 | 8.00 | 28.00 | 31.50 | 6.60 | 3.15 |
| Max | 63.40 | 10.20 | 388.00 | 31.50 | 20.00 | 3.50 |
| Std | 4.29 | 0.60 | 102.36 | 3.68 | 4.48 | 0.27 |
| CV (%) | 8.95 | 7.29 | 126.48 | 12.99 | 59.42 | 8.98 |
| **Parameter** | **Water to Binder Ratio** | **Water to Cement Ratio** | **Water** | **Sand Ratio** | **Slump** | **Cubic Compressive Strength of Concrete *** |
| Unit | [-] | [-] | kg/m$^3$ | % | mm | MPa |
| Notation | $I_7$ | $I_8$ | $I_9$ | $I_{10}$ | $I_{11}$ | Y |
| Min | 0.25 | 0.31 | 120.00 | 28.00 | 11.00 | 19.00 |
| Average | 0.43 | 0.46 | 175.49 | 37.23 | 98.34 | 55.80 |
| Median | 0.45 | 0.45 | 180.00 | 36.00 | 70.00 | 56.45 |
| Max | 0.69 | 0.69 | 291.00 | 44.00 | 260.00 | 96.30 |
| Std | 0.09 | 0.07 | 15.16 | 4.00 | 66.64 | 16.70 |
| CV (%) | 20.81 | 14.42 | 8.64 | 10.74 | 67.77 | 29.93 |

* Cylinder compressive strength = 0.82 × Cubic compressive strength.

### *3.5. Quality Assessment Criteria*

In this study, three common-used quality assessment criteria such as R, MAE and RMSE were calculated to evaluate the prediction performance of the models. Detailed information and formulations of these criteria could be found in the literature [84–91].

## 4. Results and Discussions

### *4.1. PCA's Results*

Table 2 indicates the results of PCA, including: (i) the contribution of 11 inputs to 11 principal components (denoted by $PC_k$ with k = 1:11); (ii) the explained variance (EV) of each $PC_k$ and (iii) the cumulative sum (CS) of explained variance, respectively. It can be seen that $PC_1$ exhibits 29.71% and the first 9 $PC_s$ expose 98.94% of total variance. The higher explained variance, the more statistical

information of the input space is propagated. The PCA pre-processed dataset was then created for training the models together with raw inputs.

**Table 2.** Principal Component Analysis (PCA's) results. Principal Component Analysis (PCA)

| Input | $PC_1$ | $PC_2$ | $PC_3$ | $PC_4$ | $PC_5$ | $PC_6$ | $PC_7$ | $PC_8$ | $PC_9$ | $PC_{10}$ | $PC_{11}$ |
|---|---|---|---|---|---|---|---|---|---|---|---|
| $I_1$ | 14.02 | 5.43 | 17.64 | 0.92 | 12.21 | 0.24 | 0.18 | 2.43 | 2.92 | 8.73 | 35.28 |
| $I_2$ | 11.81 | 4.96 | 26.94 | 0.00 | 5.63 | 1.38 | 0.00 | 0.05 | 2.70 | 12.69 | 33.85 |
| $I_3$ | 3.57 | 1.07 | 3.60 | 40.88 | 36.66 | 0.86 | 0.34 | 10.97 | 1.84 | 0.21 | 0.00 |
| $I_4$ | 18.43 | 1.64 | 0.81 | 1.73 | 5.55 | 2.68 | 1.27 | 61.74 | 2.57 | 0.05 | 3.53 |
| $I_5$ | 10.04 | 0.58 | 3.31 | 10.17 | 2.96 | 57.17 | 6.72 | 0.42 | 5.69 | 2.93 | 0.00 |
| $I_6$ | 0.09 | 1.55 | 10.78 | 42.35 | 33.39 | 3.42 | 4.56 | 0.22 | 2.40 | 1.05 | 0.19 |
| $I_7$ | 18.97 | 10.34 | 4.49 | 0.01 | 1.73 | 0.16 | 0.93 | 0.18 | 11.30 | 31.64 | 20.26 |
| $I_8$ | 6.48 | 31.74 | 0.04 | 0.06 | 0.35 | 0.91 | 1.91 | 0.07 | 15.77 | 37.60 | 5.07 |
| $I_9$ | 9.87 | 1.82 | 15.68 | 0.04 | 0.51 | 0.17 | 57.86 | 12.10 | 0.08 | 1.80 | 0.06 |
| $I_{10}$ | 1.70 | 34.07 | 2.63 | 0.85 | 0.02 | 0.96 | 0.28 | 2.83 | 51.88 | 3.23 | 1.54 |
| $I_{11}$ | 5.03 | 6.79 | 14.08 | 3.00 | 0.99 | 32.05 | 25.95 | 9.00 | 2.84 | 0.07 | 0.21 |
| EV | 29.71 | 19.71 | 14.32 | 9.80 | 7.57 | 6.60 | 5.25 | 3.69 | 2.30 | 0.90 | 0.16 |
| CS | 29.71 | 49.42 | 63.73 | 73.54 | 81.10 | 87.70 | 92.95 | 96.64 | 98.94 | 99.84 | 100.00 |

EV: explained variance (%); CS: cumulative sum (%).

### *4.2. Optimization Procedure: Determination of Optimal Population Size*

In this section, a parametric study for optimizing the number of populations of TLBO is presented. Simulations were performed using the number of populations ranging from 10 to 200 with a step of 10. Quality criteria, i.e., Correlation Coefficient (R), RMSE and MAE, were employed to identify the optimal number of population size, as shown in Figure 1a,b for R and RMSE, respectively. It should be noticed that a maximum number of iterations of 1000 was applied in the parametric study. As can be seen, an optimal number of population size of 40 was obtained, based on two assessments: (i) the values of R and RMSE at population size of 40 and (ii) the time consuming. Indeed, the higher population size used, the more computer processing time needed. Figure 2 shows the convergence of optimization cost with respect to R and RMSE using the optimal population size of 40. It is shown that 1000 iterations were relevant as the stopping criterion in order to obtain optimized results with respect to both R and RMSE.

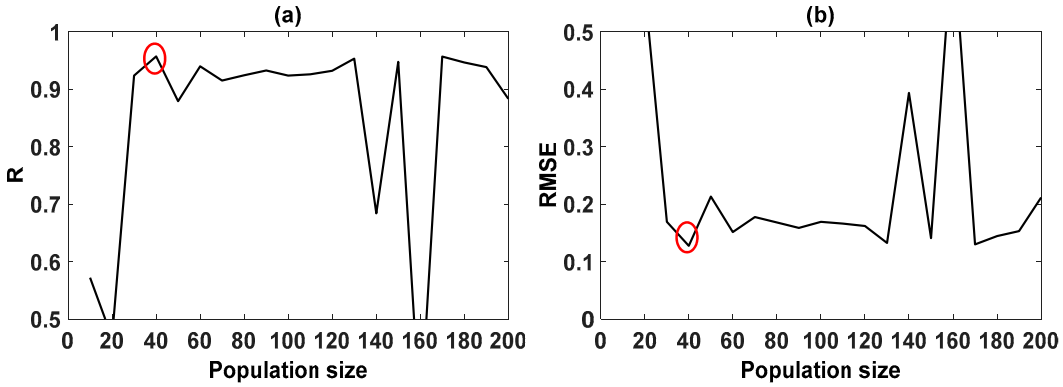


**Figure 1.** Optimization of population size with respect to (**a**) Correlation Coefficient (R) and (**b**) Root Mean Squared Error (RMSE).

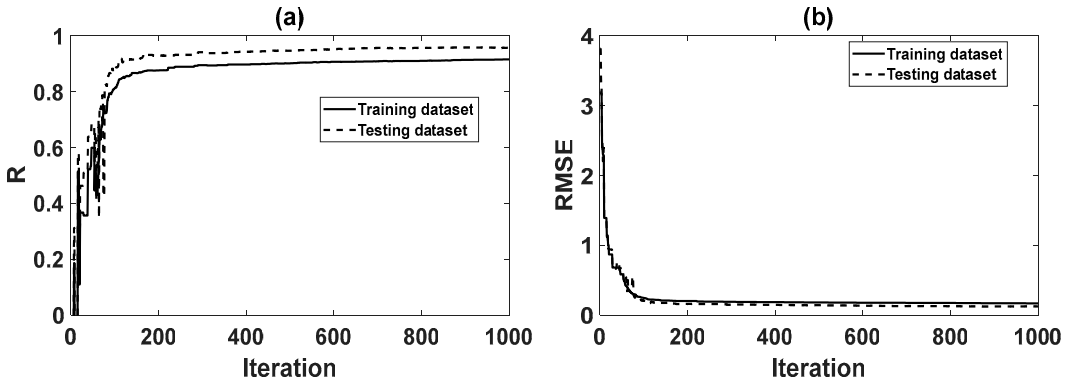


**Figure 2.** Convergence of optimization cost with respect to (**a**) R and (**b**) RMSE using a population size of 40.

### *4.3. Prediction Capability: Improvement of Single ANFIS*

In this section, the prediction capability of the proposed models is analyzed thanks to statistical error criteria such as R, RMSE and MAE. A linear fitting line, defined as "Predicted = Slope *Actual + C" is also used for the prediction capability analysis of these models. The statistical results of the ANFIS model optimized by TLBO and using PCA, denoted as ANFIS-TLBO/P, including the values of R, RMSE, MAE, error mean, error standard deviation and slope are summarized in Table 3, for the training and testing data sets. The correlation between actual and predicted compressive strength of ANFIS-TLBO/P was also plotted in Figure 3. For the training part, it can be noted that the correlation coefficient of ANFIS-TLBO/P was R = 0.92 with a slope of 0.86. For the testing part, the correlation coefficient was R = 0.96 with a slope of 0.94. In addition, the comparison of these criteria between ANFIS-TLBO/P and other models is also shown in Table 4. Let ANFIS/R and ANFIS/P are defined as the single ANFIS model using raw data and the processed data using PCA technique, respectively. Besides, the ANN model using PCA technique is designed as ANN/P, whereas ANFIS-TLBO/R is the ANFIS optimized with TLBO without the PCA treatment. In comparison with other techniques for the testing dataset, it can be seen that ANFIS-TLBO/P had the highest values of R and slope. Indeed, the value of R for ANFIS/R, ANFIS/P and ANFIS-TLBO/R was 0.86, 0.88 and 0.93, respectively. On the other hand, the value of slope for these three models was 0.78, 0.76 and 0.89, respectively.

**Table 3.** Summary information of ANFIS-TLBO/P model after using PCA. Adaptive Neuro Fuzzy Inference System (ANFIS) . Teaching-Learning-Based Optimization (TLBO). Principal Component Analysis (PCA). Mean Absolute Error (MAE).

| Criteria | Training Dataset | Testing Dataset |
|---|---|---|
| R | 0.92 | 0.96 |
| RMSE | 6.62 | 4.93 |
| MAE | 4.77 | 4.09 |
| Error mean | −0.08 | 0.26 |
| Error Std | 6.64 | 4.95 |
| Slope | 0.86 | 0.94 |

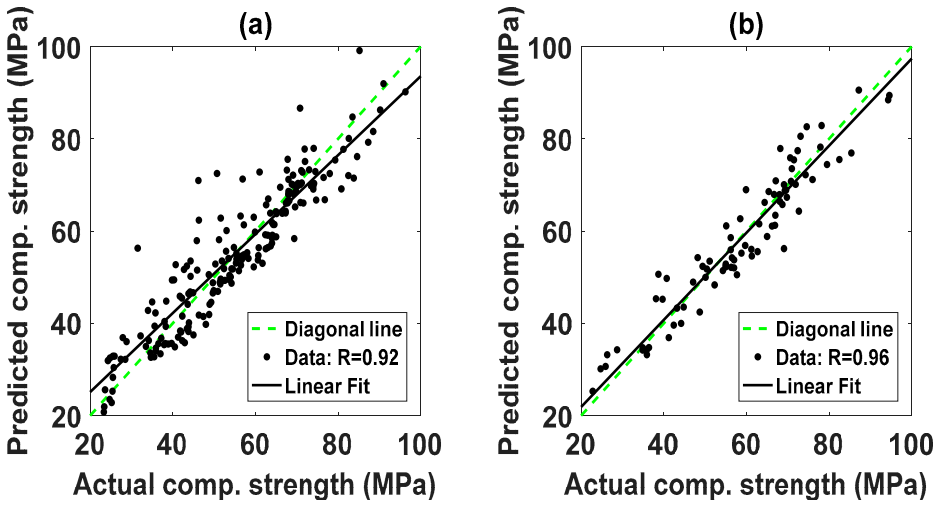


**Figure 3.** Regression graphs of ANFIS-TLBO/P model for (**a**) training and (**b**) testing dataset, respectively.

Considering now RMSE and MAE, it can be seen that the values of RMSE, MAE, error mean and error standard deviation of ANFIS-TLBO/P were 6.62, 4.77, −0.08 and 6.64, respectively for the training part; and 4.93, 4.09, 0.26 and 4.95, respectively, for the testing part. In comparison with other models with respect to the testing part, ANFIS-TLBO/P produced the highest performance, meaning the lowest values of RMSE, MAE and error standard deviation. In particular, the values of these criteria were 8.58, 6.24 and 8.63 for ANFIS/R; 7.65, 5.02 and 7.59 for ANFIS-TLBO/R; and 6.46, 5.28 and 6.49 for ANFIS/P, respectively. In addition, ANN/P was also applied to check the performance of the ANFIS-TLBO/P model and the results show that ANFIS-TLBO/P outperforms ANN/P (Table 4).

**Table 4.** Comparison of prediction capability of different models using raw and pre-processed data, respectively. Correlation Coefficient (R), Root Mean Squared Error (RMSE)

| Model | Data Used | Designation | R | RMSE | MAE | Error Std | Slope |
|---|---|---|---|---|---|---|---|
| Individual ANFIS | raw | ANFIS/R | 0.86 | 8.58 | 6.24 | 8.63 | 0.78 |
| Individual ANFIS | pre-processed | ANFIS/P | 0.93 | 6.46 | 5.28 | 6.49 | 0.89 |
| Individual ANN | pre-processed | ANN/P | 0.90 | 7.67 | 5.06 | 7.67 | 0.77 |
| ANFIS+TLBO | raw | ANFIS-TLBO/R | 0.88 | 7.65 | 5.02 | 7.59 | 0.76 |
| ANFIS+TLBO | pre-processed | ANFIS-TLBO/P | **0.96** | **4.93** | **4.09** | **4.95** | **0.94** |

For conclusion, firstly, PCA technique helped increasing the prediction performance of the AI models by reducing noise in the input space. Secondly, TLBO technique well optimized the parameters of individual the models. Finally, out of all tested models, ANFIS-TLBO/P was the best model for the prediction of MSC compressive strength, in taking into account sand's characteristics.

### *4.4. Sensitivity Analysis*

In this section, the influence of Principal Components (PCs) as well as inputs on the prediction of compressive strength of MSC is analyzed. The influence is characterized by the sensitivity index (in %), which was calculated based on various levels of variables from quantiles 0 to 100%. Details of the calculation could be found in the literature [61,92]. Figure 4a, 4b show the sensitivity index of 11 PCs and inputs, respectively, in a descending order. All explicit values are indicated in Table 5. It should be noticed that the contribution of each inputs on PCs was indicated in Table 2.

Figure 4b shows that the most three distinguished important input are curing age ($I_3$), following by fineness modulus of sand ($I_6$) and maximum diameter of crushed stone ($I_4$). The sand ratio ($I_{10}$), compressive strength of cement at 28 days ($I_1$), water to cement ratio ($I_8$), tensile strength of cement at 28 days ($I_2$) and water to binder ratio ($I_7$) form the second group of degree of importance. The last three inputs, such as slump ($I_{11}$), stone powder content in sand ($I_5$) and water ($I_9$), each contributes at least 5% for the compressive strength of MSC.

**Table 5.** Sensitivity index of Principal Components (PCs) and Inputs, respectively.

| **PCs** | **$PC_1$** | **$PC_2$** | **$PC_3$** | **$PC_4$** | **$PC_5$** | **$PC_6$** | **$PC_7$** | **$PC_8$** | **$PC_9$** | **$PC_{10}$** | **$PC_{11}$** |
|---|---|---|---|---|---|---|---|---|---|---|---|
| Sensitivity index (%) | 12.48 | 17.04 | 10.53 | 17.41 | 15.16 | 1.80 | 0.72 | 11.68 | 4.37 | 3.85 | 4.95 |
| **Inputs** | **$I_1$** | **$I_2$** | **$I_3$** | **$I_4$** | **$I_5$** | **$I_6$** | **$I_7$** | **$I_8$** | **$I_9$** | **$I_{10}$** | **$I_{11}$** |
| Sensitivity index (%) | 9.04 | 8.32 | 15.07 | 11.36 | 5.41 | 14.12 | 7.61 | 8.71 | 5.19 | 9.27 | 5.89 |

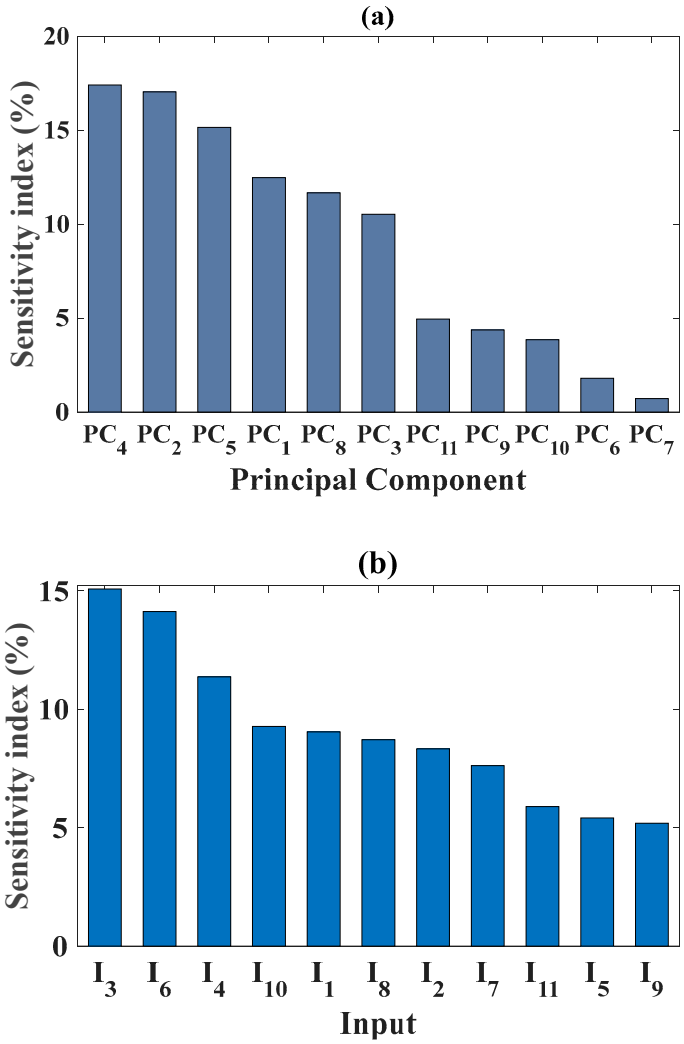


**Figure 4.** Sensitivity index of (**a**) PCs and (**b**) Inputs.

### *4.5. Comparison with Existing Models in the Literature*

In this section, the prediction performance of ANFIS-TLBO/P model is compared with existing formula in literature. In the work of Ding et al. [14], an empirical equation has been proposed in order to estimate the MSC compressive strength based on the cement compressive strength at 28 days, the

cement density and the water to cement ratio. Table 6 indicates the value of performance indicators such as R, RMSE, MAE, Error standard deviation and slope, using ANFIS-TLBO/P and the formula proposed by Ding et al. [14]. The comparison is presented for 7, 28, 56 and all curing age, respectively. For other curing ages such as 14, 60, 70, 84, 90 and 180, the number of samples is lower than 10 and thus not be considered in the comparison. In Table 6, Δ is the deviation (in %) of performance indicators between the present work ANFIS-TLBO/P model and Ding et al. [14]. Noting that the values of Δ with respect to R and slope were calculated based on the deviation around 1, whereas the values of Δ corresponding to RMSE, MAE and Error Std were computed based on changes regarding zero, as indicated by the following equation:

$$\Delta = \begin{cases} \left( (\lambda^{\text{our-model}} - 1) - (\lambda^{\text{original-model}} - 1) \right) \times 100 & \text{in case of: R, Slope} \\ \left( (\lambda^{\text{our-model}} - \lambda^{\text{other-model}}) / \lambda^{\text{original-model}} \right) \times 100 & \text{in case of: RMSE, MAE and Error}_{\text{std}} \end{cases} \quad (5)$$

**Table 6.** Comparison between ANFIS-TLBO/P and existing formula in the literature.

| Curing Age | Model | R | RMSE | MAE | Error Std | Slope |
|---|---|---|---|---|---|---|
| 7 days | Ding et al. [14] (Equation (6) *) | 0.61 | 14.42 | 10.25 | 10.41 | 1.77 |
| | Our model | 0.90 | 7.43 | 5.22 | 6.06 | 0.99 |
| | Δ (%) | +29.00 | +48.49 | +49.03 | +41.78 | +76.00 |
| 28 days | Ding et al. [14] (Equation (5)) | 0.92 | 5.31 | 4.44 | 5.32 | 0.94 |
| | Our model | 0.95 | 5.20 | 4.08 | 5.18 | 0.87 |
| | Δ (%) | +3.00 | +2.07 | +8.11 | +2.63 | −7.00 |
| 56 days | Ding et al. [14] (Equation (6) *) | 0.91 | 6.36 | 3.90 | 5.38 | 0.68 |
| | Our model | 0.87 | 5.94 | 5.43 | 4.46 | 0.83 |
| | Δ (%) | −4.00 | +6.53 | −39.23 | +17.01 | +15.00 |
| 3–388 days | Ding et al. [14] (Equation (6) *) | 0.77 | 12.82 | 9.96 | 12.54 | 0.66 |
| | Our model | 0.93 | 6.16 | 4.57 | 6.17 | 0.88 |
| | Δ (%) | +16.00 | +51.92 | +54.11 | +50.76 | +22.00 |

* a coefficient of c = 0.3 was used according to [82].

In cases of curing age of 7 and 28 days, the developed ANFIS-TLBO/P model provided better performance indicators than the proposed exponential functions in Ding et al. [14]. In case of curing age of 56 days, negative effects were observed regarding to R and MAE. However, in terms of RMSE, error Std and slope, the proposed model gave the better prediction performance. Overall, from 3–388 days of curing age, the proposed ANFIS-TLBO/P model outperforms the empirical formulas in Ding et al. [14], with respect to R, RMSE, MAE, error Std and slope. It is worth noticed that Ding et al. [14] have optimized their equations based on only three variables, such as cement compressive strength at 28 days, cement density and water to cement ratio. Other factors have not been considered in the exponential equation form. Consequently, the influence of sand's characteristic, especially stone powder content, have not been investigated. In addition, it is worth mentioned that as reported in Shen et al. [13], stone powder content in sand had a major effect on the compressive strength of MSC. Moreover, the impact of other sand's characteristics on the compressive behavior of MSC is also discussed in the works of Nanthagopalan et al. [1] and Ji et al. [2]. In short, the ANFIS-TLBO/P model developed in this study provided better prediction capability of compressive strength of MSC than other approaches and models in taking into account the variation of sand's characteristics in the simulation.

## 5. Conclusions

In this study, two optimized soft computing techniques such as PCA and TLBO were applied to improve the performance of individual ANFIS model for predicting the compressive strength of MSC. A number of 289 experimental tests of MSC were used as dataset for the simulation including

inputs parameters such as mixture proportions, cement's compressive strength, water content as well as manufactured sand's characteristics. Various validation criteria such as R, RMSE and MAE were employed to validate and test the performance of the proposed model, as well as to compare with other AI models such as individual ANFIS and ANN with or without PCA treatment. Based on the results of this study, several conclusions could be deduced: (i) data pre-processing technique such as PCA is indispensable in order to improve the prediction capability of the AI models; (ii) TLBO algorithm exhibited a strong efficiency in finding the optimal parameters of individual ANFIS model; (iii) hybrid ANFIS-TLBO/P model is the best model for predicting compressive strength of MSC in compared to other models; and (iv) sand's characteristics should be integrated in the input space for the simulation of the AI models for predicting the MSC compressive strength.

In terms of perspectives, uncertainty quantification should also be addressed for quantifying the confidence interval of MSC's compressive behavior in the presence of input variability.

**Author Contributions:** Conceptualization, H.B.L. and T.T.L.; Methodology, H.B.L., L.M.L. and T.T.L.; Software, H.B.L. and T.T.L.; Validation, H.B.L., V.M.L. and B.T.P.; Formal Analysis, L.M.L. and T.T.L.; Investigation, H.B.L. and D.V.D. and B.T.P.; Resources, V.M.L.; Data Curation, V.M.L. and B.T.P.; Writing-Original Draft Preparation, H.B.L., V.M.L., T.T.L., and B.T.P.; Writing-Review & Editing, H.B.L., L.M.L., T.T.L. and B.T.P.; Visualization, H.B.L. and B.T.P.; Supervision, H.B.L., D.V.D. and B.T.P.; Project Administration, L.M.L., T.T.L. and B.T.P.; Funding Acquisition, B.T.P.

**Conflicts of Interest:** The authors declare no conflict of interest.

## Abbreviations

| Designation | Explanation |
|---|---|
| MSC | Manufactured Sand Concrete |
| ANFIS | Adaptive Neuro Fuzzy Inference System |
| ANN | Artificial Neural Networks |
| SVM | Support Vector Machine |
| FL | Fuzzy Logic |
| TLBO | Teaching-Learning-Based Optimization |
| PCA | Principal Component Analysis |
| $PC_k$ (k = 1:11) | Principal components |
| EV | Explained variance |
| CS | Cumulative sum |
| AI | Artificial Intelligence |
| R | Correlation Coefficient |
| RMSE | Root Mean Squared Error |
| MAE | Mean Absolute Error |
| Std | Standard deviation |
| $I_i$ (I = 1:11) | Designation of inputs |
| Y | Designation of target |

## 1. References

1. Nanthagopalan, P.; Santhanam, M. Fresh and hardened properties of self-compacting concrete produced with manufactured sand. *Cem. Concr. Compos.* **2011**, *33*, 353–358.
2. Ji, T.; Chen, C.-Y.; Zhuang, Y.-Z.; Chen, J.-F. A mix proportion design method of manufactured sand concrete based on minimum paste theory. *Constr. Build. Mater.* **2013**, *44*, 422–426.
3. Shen, W.; Yang, Z.; Cao, L.; Cao, L.; Liu, Y.; Yang, H.; Lu, Z.; Bai, J. Characterization of manufactured sand: Particle shape, surface texture and behavior in concrete. *Constr. Build. Mater.* **2016**, *114*, 595–601.
4. Swamy, R.N. *The Alkali-Silica Reaction in Concrete*; CRC Press: Boca Raton, FL, USA, 2002.
5. Zhao, S.B.; Ding, X.X.; Li, C.Y. Bond-Slip Relation of Plain Steel Bar in Concrete with Machine-Made Sand. Available online: https://www.scientific.net/AMM.238.142 (accessed on 5 July 2019).

6. Li, B.; Ke, G.; Zhou, M. Influence of manufactured sand characteristics on strength and abrasion resistance of pavement cement concrete. *Constr. Build. Mater.* **2011**, *25*, 3849–3853.
7. Gonçalves, J.; Tavares, L.; Filho, R.T.; Fairbairn, E.; Cunha, E. Comparison of natural and manufactured fine aggregates in cement mortars. *Cem. Concr. Res.* **2007**, *37*, 924–932.
8. Yamei, H.; Lihua, W. Effect of Particle Shape of Limestone Manufactured Sand and Natural Sand on Concrete. *Procedia Eng.* **2017**, *210*, 87–92.
9. Mundra, S.; Sindhi, P.; Chandwani, V.; Nagar, R.; Agrawal, V. Crushed rock sand—An economical and ecological alternative to natural sand to optimize concrete mix. *Perspect. Sci.* **2016**, *8*, 345–347.
10. Guan, M.; Liu, W.; Lai, M.; Du, H.; Cui, J.; Gan, Y. Seismic behaviour of innovative composite walls with high-strength manufactured sand concrete. *Eng. Struct.* **2019**, *195*, 182–199.
11. Guan, M.; Lai, Z.; Xiao, Q.; Du, H.; Zhang, K. Bond behavior of concrete-filled steel tube columns using manufactured sand (MS-CFT). *Eng. Struct.* **2019**, *187*, 199–208.
12. Li, B.; Wang, J.; Zhou, M. Effect of limestone fines content in manufactured sand on durability of low- and high-strength concretes. *Constr. Build. Mater.* **2009**, *23*, 2846–2850.
13. Shen, W.; Liu, Y.; Wang, Z.; Cao, L.; Wu, D.; Wang, Y.; Ji, X. Influence of manufactured sand's characteristics on its concrete performance. *Constr. Build. Mater.* **2018**, *172*, 574–583.
14. Ding, X.; Li, C.; Xu, Y.; Li, F.; Zhao, S. Experimental study on long-term compressive strength of concrete with manufactured sand. *Constr. Build. Mater.* **2016**, *108*, 67–73.
15. Yang, R.; Yu, R.; Shui, Z.; Guo, C.; Wu, S.; Gao, X.; Peng, S. The physical and chemical impact of manufactured sand as a partial replacement material in Ultra-High Performance Concrete (UHPC). *Cem. Concr. Compos.* **2019**, *99*, 203–213.
16. Park, S. Study on the Fluidity and Strength Properties of High Performance Concrete Utilizing Crushed Sand. *Int. J. Concr. Struct. Mater.* **2012**, *6*, 231–237.
17. Donza, H.; Cabrera, O.; Irassar, E. High-strength concrete with different fine aggregate. *Cem. Concr. Res.* **2002**, *32*, 1755–1761.
18. Mak, S.L.; Torii, K. Strength development of high strength concretes with and without silica fume under the influence of high hydration temperatures. *Cem. Concr. Res.* **1995**, *25*, 1791–1802.
19. Armaghani, D.J.; Hatzigeorgiou, G.D.; Karamani, C.; Skentou, A.; Zoumpoulaki, I.; Asteris, P.G. Soft computing-based techniques for concrete beams shear strength. *Procedia Struct. Integr.* **2019**, *17*, 924–933.
20. Yeh, I.-C. Modeling of strength of high-performance concrete using artificial neural networks. *Cem. Concr. Res.* **1998**, *28*, 1797–1808.
21. Asteris, P.G.; Ashrafian, A.; Rezaie-Balf, M. Prediction of the compressive strength of self-compacting concrete using surrogate models. **2019**, *24*, 137–150.
22. Asteris, P.G.; Kolovos, K.G. Self-compacting concrete strength prediction using surrogate models. *Neural Comput. Applic.* **2019**, *31*, 409–424.
23. Sarir, P.; Chen, J.; Asteris, P.G.; Armaghani, D.J.; Tahir, M.M. Developing GEP tree-based, neuro-swarm, and whale optimization models for evaluation of bearing capacity of concrete-filled steel tube columns. *Eng. Comput.* **2019**, 1–19, doi:10.1007/s00366-019-00808-y.
24. Apostolopoulou, M.; Armaghani, D.J.; Bakolas, A.; Douvika, M.G.; Moropoulou, A.; Asteris, P.G. Compressive strength of natural hydraulic lime mortars using soft computing techniques. *Procedia Struct. Integr.* **2019**, *17*, 914–923.
25. Van Dao, D.; Ly, H.-B.; Trinh, S.H.; Le, T.-T.; Pham, B.T. Artificial Intelligence Approaches for Prediction of Compressive Strength of Geopolymer Concrete. *Materials* **2019**, *12*, 983.
26. Dao, D.; Trinh, S.H.; Ly, H.-B.; Pham, B.T. Prediction of Compressive Strength of Geopolymer Concrete Using Entirely Steel Slag Aggregates: Novel Hybrid Artificial Intelligence Approaches. *Appl. Sci.* **2019**, *9*, 1113.
27. Golafshani, E.M.; Behnood, A. Estimating the optimal mix design of silica fume concrete using biogeography-based programming. *Cem. Concr. Compos.* **2019**, *96*, 95–105.
28. Bingöl, A.F.; Tortum, A.; Gül, R. Neural networks analysis of compressive strength of lightweight concrete after high temperatures. *Mater. Des. (1980–2015)* **2013**, *52*, 258–264.
29. Mishra, M.; Bhatia, A.S.; Maity, D. A comparative study of regression, neural network and neuro-fuzzy inference system for determining the compressive strength of brick–mortar masonry by fusing nondestructive testing data. *Eng. Comput.* **2019**, 1–15, dio:10.1007/s00366-019-00810-4.

30. Bui, D.T.; Abdullahi, M.M.; Ghareh, S.; Moayedi, H.; Nguyen, H. Fine-tuning of neural computing using whale optimization algorithm for predicting compressive strength of concrete. *Eng. Comput.* **2019**, 1–12, doi:10.1007/s00366-019-00850-w.
31. Behnood, A.; Golafshani, E.M. Predicting the compressive strength of silica fume concrete using hybrid artificial neural network with multi-objective grey wolves. *J. Clean. Prod.* **2018**, *202*, 54–64.
32. Peng, C.-H.; Yeh, I.-C.; Lien, L.-C. Building strength models for high-performance concrete at different ages using genetic operation trees, nonlinear regression, and neural networks. *Eng. Comput.* **2010**, *26*, 61–73.
33. Tsai, H.-C.; Lin, Y.-H. Predicting high-strength concrete parameters using weighted genetic programming. *Eng. Comput.* **2011**, *27*, 347–355.
34. Yeh, I.-C. Optimization of concrete mix proportioning using a flattened simplex–centroid mixture design and neural networks. *Eng. Comput.* **2008**, *25*, 179–190.
35. Alipour, R.; Toghroli, A.; Mu'Azu, M.; Katebi, J.; Mohammadhassani, M.; Khalafi, S.; Mohamad, E.T.; Wakil, K.; Khorami, M. Computational optimized finite element modelling of mechanical interaction of concrete with fiber reinforced polymer. *Comput. Concr.* **2019**, *23*, 061.
36. Asteris, P.G.; Nikoo, M. Artificial bee colony-based neural network for the prediction of the fundamental period of infilled frame structures. *Neural Comput. Appl.* **2019**, 1–11, doi:10.1007/s00366-019-00850-w.
37. Jang, J.R. ANFIS: Adaptive-network-based fuzzy inference system. *IEEE Trans. Syst. Man Cybern.* **1993**, *23*, 665–685.
38. Nguyen, P.T.; Tuyen, T.T.; Shirzadi, A.; Pham, B.T.; Shahabi, H.; Omidvar, E.; Amini, A.; Entezami, H.; Prakash, I.; Phong, T.V. Development of a Novel Hybrid Intelligence Approach for Landslide Spatial Prediction. *Appl. Sci.* **2019**, *9*, 2824.
39. Kaloop, M.R.; Kumar, D.; Samui, P.; Gabr, A.R.; Hu, J.W.; Jin, X.; Roy, B. Particle Swarm Optimization Algorithm-Extreme Learning Machine (PSO-ELM) Model for Predicting Resilient Modulus of Stabilized Aggregate Bases. *Appl. Sci.* **2019**, *9*, 3221.
40. Xu, H.; Zhou, J.; Asteris, P.G.; Armaghani, D.J.; Tahir, M.M. Supervised Machine Learning Techniques to the Prediction of Tunnel Boring Machine Penetration Rate. *Appl. Sci.* **2019**, *9*, 3715.
41. Le, L.T.; Nguyen, H.; Dou, J.; Zhou, J. A Comparative Study of PSO-ANN, GA-ANN, ICA-ANN, and ABC-ANN in Estimating the Heating Load of Buildings' Energy Efficiency for Smart City Planning. *Appl. Sci.* **2019**, *9*, 2630.
42. Pham, B.T.; Son, L.H.; Hoang, T.-A.; Nguyen, D.-M.; Bui, D.T. Prediction of shear strength of soft soil using machine learning methods. *Catena* **2018**, *166*, 181–191.
43. Jang, J.; Sun, C.; Mizutani, E. Neuro-Fuzzy and Soft Computing-A Computational Approach to Learning and Machine Intelligence [Book Review]. *IEEE Trans. Autom. Control.* **1997**, *42*, 1482–1484.
44. Esmaeili, M.; Osanloo, M.; Rashidinejad, F.; Aghajani Bazzazi, A.; Taji, M. Multiple regression, ANN and ANFIS models for prediction of backbreak in the open pit blasting. *Eng. Comput.* **2014**, *30*, 549–558.
45. Pham, B.T.; Nguyen, M.D.; Van Dao, D.; Prakash, I.; Ly, H.B.; Le, T.T.; Ho, L.S.; Nguyen, K.T.; Ngo, T.Q.; Hoang, V.; et al. Development of artificial intelligence models for the prediction of Compression Coefficient of soil: An application of Monte Carlo sensitivity analysis. *Sci. Total. Environ.* **2019**, *679*, 172–184.
46. Pham, B.T.; Jaafari, A.; Prakash, I.; Singh, S.K.; Quoc, N.K.; Bui, D.T. Hybrid computational intelligence models for groundwater potential mapping. *Catena* **2019**, *182*, 104101.
47. Karaboga, D.; Kaya, E. Adaptive network based fuzzy inference system (ANFIS) training approaches: A comprehensive survey. *Artif. Intell. Rev.* **2018**, 1–31.
48. Le, L.M.; Ly, H.-B.; Pham, B.T.; Le, V.M.; Pham, T.A.; Nguyen, D.-H.; Tran, X.-T.; Le, T.-T. Hybrid Artificial Intelligence Approaches for Predicting Buckling Damage of Steel Columns Under Axial Compression. *Materials* **2019**, *12*, 1670.
49. Termeh, S.V.R.; Khosravi, K.; Sartaj, M.; Keesstra, S.D.; Tsai, F.T.-C.; Dijksma, R.; Pham, B.T. Optimization of an adaptive neuro-fuzzy inference system for groundwater potential mapping. *Hydrogeol. J.* **2019**, 1–24, 10.1007/s10040-019-02017-9.
50. Takagi, T.; Sugeno, M. Derivation of Fuzzy Control Rules from Human Operator's Control Actions. *IFAC Proc. Vol.* **1983**, *16*, 55–60.
51. Takagi, T.; Sugeno, M. Fuzzy Identification of Systems and Its Applications to Modeling and Control. In *Readings in Fuzzy Sets for Intelligent Systems*; Elsevier BV: Amsterdam, The Netherlands, 1993; pp. 387–403.
52. Abraham, A. Adaptation of Fuzzy Inference System Using Neural Learning. In *Granular Computing*; Springer Science and Business Media LLC: Berlin, Germany, 2005; Volume 181, pp. 53–83.

53. Nguyen, H.-L.; Le, T.-H.; Pham, C.-T.; Le, T.-T.; Ho, L.S.; Le, V.M.; Pham, B.T.; Ly, H.-B. Development of Hybrid Artificial Intelligence Approaches and a Support Vector Machine Algorithm for Predicting the Marshall Parameters of Stone Matrix Asphalt. *Appl. Sci.* **2019**, *9*, 3172.
54. Aditya, M.; Chandranath, C.; Singh, R.N. Flood Forecasting Using ANN, Neuro-Fuzzy, and Neuro-GA Models. *J. Hydrol. Eng.* **2009**, *14*, 647–652.
55. Nayak, P.C.; Sudheer, K.P.; Rangan, D.M.; Ramasastri, K.S. Short-term flood forecasting with a neurofuzzy model. *Water Resour. Res.* **2005**, *41*, 41.
56. Bui, K.-T.T.; Bui, D.T.; Zou, J.; Van Doan, C.; Revhaug, I. A novel hybrid artificial intelligent approach based on neural fuzzy inference model and particle swarm optimization for horizontal displacement modeling of hydropower dam. *Neural Comput. Appl.* **2016**, *29*, 1495–1506.
57. Bui, D.T.; Khosravi, K.; Li, S.; Shahabi, H.; Panahi, M.; Singh, V.P.; Chapi, K.; Shirzadi, A.; Panahi, S.; Chen, W.; et al. New Hybrids of ANFIS with Several Optimization Algorithms for Flood Susceptibility Modeling. *Water (MDPI)* **2018**, *10*, 1210.
58. Chen, M.-Y. A hybrid ANFIS model for business failure prediction utilizing particle swarm optimization and subtractive clustering. *Inf. Sci.* **2013**, *220*, 180–195.
59. Jaafari, A.; Panahi, M.; Pham, B.T.; Shahabi, H.; Bui, D.T.; Rezaie, F.; Lee, S. Meta optimization of an adaptive neuro-fuzzy inference system with grey wolf optimizer and biogeography-based optimization algorithms for spatial prediction of landslide susceptibility. *Catena* **2019**, *175*, 430–445.
60. Pham, B.T.; Prakash, I. Spatial Prediction of Rainfall Induced Shallow Landslides Using Adaptive-Network-Based Fuzzy Inference System and Particle Swarm Optimization: A Case Study at the Uttarakhand Area, India. In *Advances and Applications in Geospatial Technology and Earth Resources*; Springer Science and Business Media LLC: Berlin, Germany, 2017; pp. 224–238.
61. Ly, H.-B.; Le, L.M.; Duong, H.T.; Nguyen, T.C.; Pham, T.A.; Le, T.-T.; Le, V.M.; Nguyen-Ngoc, L.; Pham, B.T. Hybrid Artificial Intelligence Approaches for Predicting Critical Buckling Load of Structural Members under Compression Considering the Influence of Initial Geometric Imperfections. *Appl. Sci.* **2019**, *9*, 2258.
62. Cavaleri, L.; Asteris, P.G.; Psyllaki, P.P.; Douvika, M.G.; Skentou, A.D.; Vaxevanidis, N.M. Prediction of Surface Treatment Effects on the Tribological Performance of Tool Steels Using Artificial Neural Networks. *Appl. Sci.* **2019**, *9*, 2788.
63. Asteris, P.G.; Nozhati, S.; Nikoo, M.; Cavaleri, L.; Nikoo, M. Krill herd algorithm-based neural network in structural seismic reliability evaluation. *Mech. Adv. Mater. Struct.* **2018**, *26*, 1146–1153.
64. Rao, R.; Savsani, V.; Vakharia, D.; Savsani, V. Teaching–learning-based optimization: A novel method for constrained mechanical design optimization problems. *Comput. Des.* **2011**, *43*, 303–315.
65. Rao, R.V.; Savsani, V.J.; Vakharia, D.P. Teaching–learning-based optimization: An optimization method for continuous non-linear large scale problems. *Inf. Sci.* **2012**, *183*, 1–15.
66. Rao, R.V.; Patel, V. An elitist teaching-learning-based optimization algorithm for solving complex constrained optimization problems. *Int. J. Ind. Eng. Comput.* **2012**, *3*, 535–560.
67. Hassanzadeh, Y.; Jafari-Bavil-Olyaei, A.; Aalami, M.-T.; Kardan, N. Experimental and numerical investigation of bridge pier scour estimation using ANFIS and teaching–learning-based optimization methods. *Eng. Comput.* **2019**, *35*, 1103–1120.
68. Abhishek, K.; Kumar, V.R.; Datta, S.; Mahapatra, S.S. Application of JAYA algorithm for the optimization of machining performance characteristics during the turning of CFRP (epoxy) composites: Comparison with TLBO, GA, and ICA. *Eng. Comput.* **2017**, *33*, 457–475.
69. Cheng, M.-Y.; Prayogo, D. A novel fuzzy adaptive teaching–learning-based optimization (FATLBO) for solving structural optimization problems. *Eng. Comput.* **2017**, *33*, 55–69.
70. Bayat, M.; Ghorbanpour, M.; Zare, R.; Jaafari, A.; Pham, B.T. Application of artificial neural networks for predicting tree survival and mortality in the Hyrcanian forest of Iran. *Comput. Electron. Agric.* **2019**, *164*, 104929.
71. Jolliffe, I.T. *Principal Component Analysis; Springer Series in Statistics*, 2nd ed.; Springer: New York, NY, USA, 2002; ISBN 978-0-387-95442-4.
72. Gosav, S.; Praisler, M.; Birsa, M.L. Principal Component Analysis Coupled with Artificial Neural Networks—A Combined Technique Classifying Small Molecular Structures Using a Concatenated Spectral Database. *Int. J. Mol. Sci.* **2011**, *12*, 6668–6684.
73. Defernez, M.; Kemsley, E.K. Avoiding overfitting in the analysis of high-dimensional data with artificial neural networks (ANNs). *Analyst* **1999**, *124*, 1675–1681.

74. May, R.; Dandy, G.; Maier, H. Review of Input Variable Selection Methods for Artificial Neural Networks. *Artificial Neural Networks—Methodological Advances and Biomedical Applications*; IntechOpen Limited: London, UK, 2011.
75. Feng, S.; Zhou, H.; Dong, H. Using deep neural network with small dataset to predict material defects. *Mater. Des.* **2019**, *162*, 300–310.
76. Le, T.-T.; Guilleminot, J.; Soize, C. Stochastic continuum modeling of random interphases from atomistic simulations. Application to a polymer nanocomposite. *Comput. Methods Appl. Mech. Eng.* **2016**, *303*, 430–449.
77. Krzanowski, W.J. *Principles of Multivariate Analysis: A User's Perspective*, Revised, Subsequent ed.; Oxford University Press: New York, NY, USA, 2000; ISBN 978-0-19-850708-6.
78. Ly, H.-B.; Desceliers, C.; Le, L.M.; Le, T.-T.; Pham, B.T.; Nguyen-Ngoc, L.; Doan, V.T.; Le, M. Quantification of Uncertainties on the Critical Buckling Load of Columns under Axial Compression with Uncertain Random Materials. *Materials* **2019**, *12*, 1828.
79. Noori, R.; Sabahi, M.; Karbassi, A.; Baghvand, A.; Zadeh, H.T.; Karbassi, A. Multivariate statistical analysis of surface water quality based on correlations and variations in the data set. *Desalination* **2010**, *260*, 129–136.
80. Pham, B.T.; Jaafari, A.; Prakash, I.; Bui, D.T. A novel hybrid intelligent model of support vector machines and the MultiBoost ensemble for landslide susceptibility modeling. *Bull. Eng. Geol. Environ.* **2019**, *78*, 2865–2886.
81. Ding, X.; Li, C.; Xu, Y.; Li, F.; Zhao, S. Dataset of long-term compressive strength of concrete with manufactured sand. *Data Brief.* **2016**, *6*, 959–964.
82. Zhao, S.; Ding, X.; Zhao, M.; Li, C.; Pei, S. Experimental study on tensile strength development of concrete with manufactured sand. *Constr. Build. Mater.* **2017**, *138*, 247–253.
83. Zhao, S.; Hu, F.; Ding, X.; Zhao, M.; Li, C.; Pei, S. Dataset of tensile strength development of concrete with manufactured sand. *Data Brief.* **2017**, *11*, 469–472.
84. Cavaleri, L.; Chatzarakis, G.E.; Trapani, F.D.; Douvika, M.G.; Roinos, K.; Vaxevanidis, N.M.; Asteris, P.G. Modeling of surface roughness in electro-discharge machining using artificial neural networks. *Adv. Mater. Res.* **2017**, *6*, 169.
85. Chen, H.; Asteris, P.G.; Armaghani, D.J.; Gordan, B.; Pham, B.T. Assessing Dynamic Conditions of the Retaining Wall: Developing Two Hybrid Intelligent Models. *Appl. Sci.* **2019**, *9*, 1042.
86. Psyllaki, P.; Stamatiou, K.; Iliadis, I.; Mourlas, A.; Asteris, P.; Vaxevanidis, N. Surface treatment of tool steels against galling failure. *MATEC Web Conf.* **2018**, *188*, 04024.
87. Asteris, P.G.; Plevris, V. Anisotropic masonry failure criterion using artificial neural networks. *Neural Comput. Applic.* **2017**, *28*, 2207–2229.
88. Khozani, Z.S.; Khosravi, K.; Pham, B.T.; Kløve, B.; Mohtar, W.H.M.W.; Yaseen, Z.M. Determination of compound channel apparent shear stress: Application of novel data mining models. *J. Hydroinformatics* **2019**.
89. Pham, B.T.; Nguyen, M.D.; Bui, K.-T.T.; Prakash, I.; Chapi, K.; Bui, D.T. A novel artificial intelligence approach based on Multi-layer Perceptron Neural Network and Biogeography-based Optimization for predicting coefficient of consolidation of soil. *Catena* **2019**, *173*, 302–311.
90. Zhou, J.; Nekouie, A.; Arslan, C.A.; Pham, B.T.; Hasanipanah, M. Novel approach for forecasting the blast-induced AOp using a hybrid fuzzy system and firefly algorithm. *Eng. Comput.* **2019**, 1–10.
91. Nguyen, M.D.; Pham, B.T.; Tuyen, T.T.; Hai Yen, H.P.; Prakash, I.; Vu, T.T.; Chapi, K.; Shirzadi, A.; Shahabi, H.; Dou, J.; et al. Development of an Artificial Intelligence Approach for Prediction of Consolidation Coefficient of Soft Soil: A Sensitivity Analysis. *Open Constr. Build. Technol. J.* **2019**, 13, doi: 10.1016/j.scitotenv.2019.05.061.
92. Ly, H.-B.; Monteiro, E.; Le, T.-T.; Le, V.M.; Dal, M.; Regnier, G.; Pham, B.T. Prediction and Sensitivity Analysis of Bubble Dissolution Time in 3D Selective Laser Sintering Using Ensemble Decision Trees. *Materials* **2019**, *12*, 1544.